Research Square

Preprints are preliminary reports that have not undergone peer review.
They should not be considered conclusive, used to inform clinical practice,
or referenced by the media as validated information.

SAR-Based Decadal Surface Water Dynamics in Bangladesh Using a Spatiotemporally Adaptive Gaussian Mixture Model (ST-GMM)

Milon Bokshi

mbokshi45@gmail.com

ICT, GIS & Remote Sensing Division, Institute of Water Modelling (IWM)

Drubo Paul

ICT, GIS & Remote Sensing Division, Institute of Water Modelling (IWM)

Md. Munir Mahmud

Institute of Remote Sensing and GIS, Jahangirnagar University

Article

Keywords: SAR, Surface water dynamics, Adaptive Thresholding, Water Mapping, Sustainable Water Resources

Posted Date: May 27th, 2026

DOI: https://doi.org/10.21203/rs.3.rs-9658329/v1

License: This work is licensed under a Creative Commons Attribution 4.0 International License.
Read Full License

Additional Declarations: No competing interests reported.

Title

SAR-Based Decadal Surface Water Dynamics in Bangladesh Using a Spatiotemporally Adaptive Gaussian Mixture Model (ST-GMM)

Authors

Milon Bokshi [1, 2, *]

Drubo Paul [2]

Md. Munir Mahmud [2, 3]

Affiliations

[1] Institute of Remote Sensing and GIS, Jahangirnagar University, Dhaka, Bangladesh

[2] ICT, GIS & Remote Sensing Division, Institute of Water Modelling (IWM), Dhaka, Bangladesh

[3] Department of Geography and Environmental Studies, Texas State University, Texas, USA

*** Corresponding author**

Email: mbokshi45@gmail.com

SAR-Based Decadal Surface Water Dynamics in Bangladesh Using a Spatiotemporally Adaptive Gaussian Mixture Model (ST-GMM)

ABSTRACT

Surface water dynamics are critical to Bangladesh's hydro-ecological systems, yet persistent monsoon cloud cover limits optical remote sensing. This study presents an 11-year (2015–2025) Sentinel-1 SAR time-series analysis (7,891 scenes) for monthly surface water monitoring using a Spatiotemporally Adaptive Gaussian Mixture Model (ST-GMM). The framework dynamically models land–water backscatter distributions to derive optimal thresholds under varying hydro-climatic conditions, addressing the "missing monsoon" problem. Results reveal a ~2.4-fold seasonal expansion from ~15,900 km² (dry season) to ~37,500 km² (monsoon). Trend analysis (Modified Mann-Kendall) indicates no significant long-term change ($\tau = -0.091$, $p = 0.76$), though a non-significant negative tendency (−342.4 km²/year) is observed. Validation against 4,310 field observations achieved 92.55% accuracy ($\kappa = 0.85$), with cross-sensor agreement of 97.9% (IoU = 0.896). The results establish a robust baseline for distinguishing natural hydrological variability from anthropogenic change and support transboundary water management in deltaic systems.

Keywords SAR, Surface water dynamics, Adaptive Thresholding, Water Mapping, Sustainable Water Resources

1 Introduction

Surface water is a dynamic component of the hydrological cycle, with pronounced temporal and spatial variability in low-lying deltaic regions. Bangladesh, situated at the confluence of the Ganges–Brahmaputra–Meghna (GBM) river system, is the world's largest delta system. Approximately 80% of the country is flood-prone, and surface water conditions directly influence agriculture, fisheries, navigation, drinking water supply, and ecosystem services for over 170 million inhabitants.[1–3]

Remote sensing provides the only feasible means for systematic, large-scale surface water monitoring. Optical sensors such as Landsat and Sentinel-2 have been widely used for water mapping;[4,5] however, their utility over Bangladesh is severely constrained during the monsoon season (June–September), when cloud cover exceeds 80% on most acquisition dates.[6,7] Synthetic Aperture Radar (SAR), operating in the microwave spectrum, overcomes this limitation by providing all-weather, day-night imaging capability. Sentinel-1 C-band SAR, in particular, has become a primary data source for surface water detection due to its free availability, systematic global coverage, and well-characterized backscatter response over water surfaces.[8–10]

SAR-based water detection exploits the specular reflection properties of smooth water surfaces, which produce characteristically low radar backscatter compared to surrounding land. Numerous studies have demonstrated the effectiveness of VV-polarized backscatter thresholding for water delineation.[9,11,12] However, the majority of SAR-based studies focus on event-specific flood mapping—detecting inundation from individual flood events—rather than characterizing long-term surface water dynamics, seasonal patterns, and inter-annual trends.[13] Recent advancements, such as the NASA JPL Dynamic Surface Water Extent (DSWx-S1) product[14] and automated recursive classification frameworks,[15,16] highlight the growing importance of operational SAR-based water monitoring. Furthermore, most approaches employ static backscatter thresholds, which may not adequately represent the seasonal variability in SAR response caused by changes in wind conditions, vegetation phenology, and soil moisture across Bangladesh's four distinct

hydrological seasons. Tran et al.[17] recently demonstrated the utility of Sentinel-1 time series for monitoring dynamic deltas, further justifying the need for adaptive monitoring frameworks.

This study addresses these gaps by presenting a comprehensive decadal-scale analysis of surface water dynamics across Bangladesh using Sentinel-1 SAR data from 2015 to 2025. The specific objectives are to propose a threshold-based spatiotemporally adaptive probabilistic framework (ST-GMM) to dynamically model land–water backscatter distributions across diverse hydrological regimes, and to systematically quantify multi-decadal surface water changes, seasonal variability, and long-term trends across Bangladesh using robust non-parametric statistics. The study contributes a novel spatiotemporally adaptive probabilistic framework for robust SAR water detection, the first decadal Sentinel-1 SAR water archive for Bangladesh, an explicit cross sensor benchmarking against optical baselines (JRC GSW), and a fully reproducible cloud-based computational workflow.

2 Materials and methods

2.1 Study area

Bangladesh is located in South Asia between latitudes 20°34′ and 26°38′ N and longitudes 88°01′ and 92°41′ E, covering approximately 147,570 km^2 (**Figure 1**). The country is characterized by predominantly flat topography, dense river networks, and extensive floodplains formed by the Ganges–Brahmaputra– Meghna (GBM) river system—the world's largest delta formation. Elevation ranges from sea level in the southern coastal zone to approximately 1,000 m in the Chittagong Hill Tracts.

Bangladesh experiences a tropical monsoon climate characterized by four distinct hydrological seasons. The Dry Winter (December–February) brings minimal rainfall and reduced river discharge, resulting in the minimum surface water extent. The Pre-Monsoon season (March–May) is marked by rising temperatures, occasional thunderstorms, and a gradual increase in water extent. The Monsoon (June–September) delivers 70–80% of annual precipitation, triggering peak river discharge and establishing the maximum surface water extent. Finally, the Post-Monsoon period (October–November) involves a steady recession of floodwaters and the gradual contraction of water bodies.

Administratively, the country comprises 8 divisions and 64 districts. This study utilizes this administrative hierarchy for multi-scale spatial analysis of surface water dynamics.



Figure 1. Map shows Bangladesh highlighting the principal river systems (Ganges, Brahmaputra, and Meghna), and the regional geographic context of the study domain.

2.2 Data and processing

Sentinel-1 C-band SAR Ground Range Detected (GRD) imagery acquired in Interferometric Wide (IW) swath mode was used as the primary data source. The VV polarization channel was selected due to its well-documented sensitivity to open water surfaces.[9,11] Detailed sensor specifications and annual scene counts are provided in Supplementary Tables S1 and S2. All SAR data processing, water detection, and product generation were performed in Google Earth Engine (GEE),[18] enabling cloud-based access to the complete Sentinel-1 archive without local data storage or computational infrastructure requirements.

To strictly quantify classification veracity independent of self-referential benchmarks, probability-based stratified random sampling was employed across the 11-year baseline. A set of 500 geographically target hubs were evenly dispersed across historical permanence classes, yielding 4,310 spatially referenced field observations representing $W \in \{0,1\}$. These points were post-stratified using the long-term Water Occurrence Layer (F) to ensure representative coverage across hydrological extremes: 700 points (16.2%) represented permanent water bodies ($F \geq 0.8$), 700 points (16.2%) represented semi-permanent water ($0.4 < F \leq 0.8$), and 528 points (12.3%) represented ephemeral floods ($F \leq 0.4$), while 2,382 points (55.3%) represented diverse non-water land cover. Baseline fidelity was established via unambiguous on-site verification and multi-temporal cross sensor confirmation.

Prior to statistical analysis, the multi-year raw dataset underwent a rigorous quality audit and standardization procedure. Initial exploration revealed a temporal data gap in January 2016, where 30 districts exhibited zero water area. This anomaly was attributed to the limited orbital coverage of Sentinel1A during its early mission phase (prior to the launch of Sentinel-1B). To maintain statistical continuity for decadal trend analysis, linear interpolation between December 2015 and February 2016 was applied to these data voids for each affected district, preserving local temporal context rather than relying on a generalized decadal mean. Trend analysis results were verified with and without these interpolated months and showed negligible differences. Furthermore, administrative naming collisions between Divisions and Districts (e.g., Barishal, Dhaka) were resolved by standardizing labels through a specialized pre-processing script to ensure accurate multi-scale reporting.

2.3 Framework and analysis

The proposed analytical framework (**Figure 2**) consists of five main components: (1) SAR-based monthly surface water detection using seasonally adaptive thresholds; (2) annual water occurrence frequency mapping; (3) inter-annual change detection for gain, loss, and stable classifications; (4) seasonal water footprint analysis; and (5) decadal trend analysis at multiple administrative scales.

To determine the optimal diagnostic threshold (τ) following the extraction of monthly regional backscatter histograms, we propose a Spatiotemporally Adaptive Gaussian Mixture Model (ST-GMM) framework. Unlike static or unconstrained thresholding methods (e.g., Otsu), the ST-GMM dynamically models the land–water backscatter distribution (σ^0) for every district d and every month t over the decadal archive. The bimodal distribution is modeled as a mixture of two Gaussian components, a choice specifically adopted to represent the fundamental land–water contrast while avoiding the over-parameterization associated with higher-order mixtures.

The probabilistic state of the system is defined by the parameter vector $\theta_{dt} = \{\pi_W, \mu_W, \sigma_W^2, \pi_L, \mu_L, \sigma_L^2\}_{dt}$, where π_{dt} represents the mixing coefficients (priors), and μ_{dt}, σ_{dt}^2 are the mean and variance. The overall probability density function is given below.

$$p(x \mid \theta_{dt}) = \pi_{W,dt}\, \mathcal{N}(x \mid \mu_{W,dt}, \sigma^2_{W,dt}) + \pi_{L,dt}\, \mathcal{N}(x \mid \mu_{L,dt}, \sigma^2_{L,dt}) \quad (1)$$

Optimization of the bi-modal mixture (**Figure 3**) is achieved over three logical steps; initially, we implement an initialization via the NDWI bridge. In complex deltaic environments where class priors (π_{dt}) shift drastically—from < 5% in the dry season to > 50% during the monsoon—unsupervised EM often suffers from initialization bias. This is resolved by an auxiliary probabilistic bridge where independent NDWI-derived masks from cloud-free optical windows (Sentinel-2 MSI) are utilized exclusively to initialize the starting class means ($\mu_{k,dt}$) and mixing coefficients ($\pi_{k,dt}$). This anchor ensures the algorithm begins near the global maximum of the parameter space. Subsequently, the EM algorithm refines the Gaussian parameters using SAR backscatter alone, ensuring the study remains operationally robust during the monsoon season when cloud cover consistently exceeds 80%, rendering optical masking ineffective.[12] The iterative process alternates between the Expectation (E) step—computing posterior probabilities for each pixel—and the Maximization (M) step—updating the distribution parameters based on the high-resolution radar return. Finally, for optimal threshold determination, the diagnostic threshold (τ_{dt}) is mathematically defined as the precise intersection point of the fitted land and water Gaussian density curves. This decision boundary is physically justified by the fundamental contrast between the specular reflection of smooth water surfaces (low backscatter) and the diffuse scattering of land surfaces (high backscatter), representing the point of minimum total classification error. This intersection approach is consistent with established operational standards such as the NASA DSWx-S1 product and earlier automated SAR thresholding frameworks.[9,12] Convergence was defined as a relative change in log-likelihood below 10^{-3}, with 100% convergence achieved across all 768 district-month combinations to provide a statistically objective and reproducible solution.

Binary surface water masks (W_{dt}) were derived by integrating the probabilistic ST-GMM threshold (τ_{dt}) with a deterministic physical constraint to eliminate systemic geographic artifacts. Specifically, topographical slope (ξ) derived from the SRTM 30m DEM was utilized to neutralize radar-shadowing effects—common in high-relief terrain like the Chittagong Hill Tracts where steep slopes mimic low return water using:[9]

$$W_{dt} = \begin{cases} 1 \text{ if } \sigma^0_{dt} \le \tau_{dt} \text{ and } \xi \le 5^\circ \\ 0 \text{ otherwise} \end{cases} \quad (2)$$

By strictly clamping inundation to pixels where the local slope does not exceed 5°, the framework filters out topographical commission errors while preserving true estuarine and floodplain features. This logical integration ensures that only geographically plausible depressions are mapped as water bodies, combining backscatter-based evidence with terrain-based constraints for maximum classification reliability.

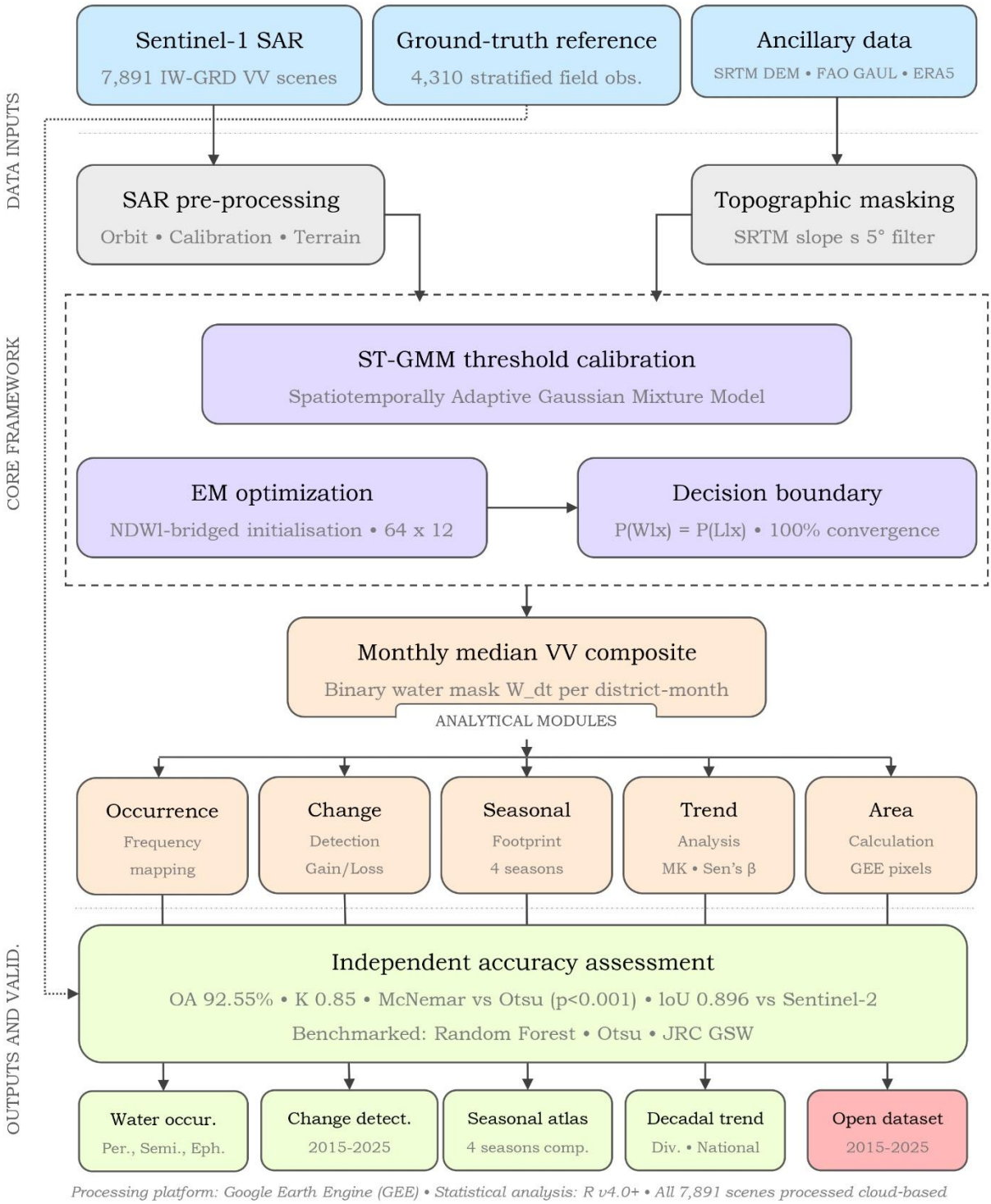


Figure 2. Methodological framework for decadal surface water monitoring in Bangladesh using Spatiotemporally Adaptive Gaussian Mixture Modeling (ST-GMM).

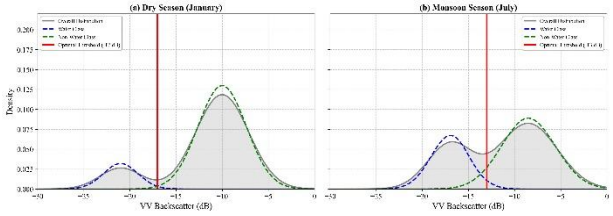


Figure. 3. Representative bimodal distributions of Sentinel-1 VV backscatter for (a) the dry season (January) and (b) the monsoon season (July). The vertical lines indicate the GMM-calibrated optimal thresholds (−17.5 dB and −13.8 dB), representing the point of minimum total classification error for each respective season.

Following the generation of the primary binary mask time-series, three higher-order analytical products were derived to characterize the hydrological regime. Initially, annual water occurrence frequency (F) was computed as the cumulative count of months in which a pixel was classified as surface water:

$$F = \sum_{m=1}^{12} W_m \qquad (3)$$

where F ranges from 0 (never water) to 12 (water in all months). Based on this metric, surface water bodies are analytically partitioned into three hydrologically meaningful persistence classes. Permanent water ($F \geq 10$) corresponds primarily to major river channels, large lakes, and deep reservoirs that maintain open water in nearly every month of the year; the threshold is set slightly below 12 to explicitly account for occasional missing satellite acquisitions or wind-induced surface roughening that may momentarily disrupt an otherwise perennial water signature. Semi-permanent water ($5 \leq F < 10$) captures dynamic floodplains, seasonal wetlands, and shallow water bodies that are inundated for a significant portion of the year but recede during the dry season. Ephemeral water ($1 \leq F < 5$) delineates zones of temporary inundation driven primarily by intense monsoon precipitation and transboundary discharge pulses, including shallow agricultural flooding and short-duration ponding.

To quantify surface water flux across the decadal observation period, inter-annual change mapping between two years (Y_1 and Y_2) was implemented for four distinct categories:

$$\text{Change} = \begin{cases} \text{Gained} & \text{if } WY1 = 0 \text{ and } WY2 = 1 \\ \text{Lost} & \text{if } WY1 = 1 \text{ and } WY2 = 0 \\ \text{Stable} & \text{if } WY1 = 1 \text{ and } WY2 = 1 \\ \text{No Water} & \text{if } WY1 = 0 \text{ and } WY2 = 0 \end{cases} \qquad (4)$$

Change maps were generated for two key temporal windows; the full decadal comparison (2015 vs. 2025) and a more recent five-year comparison (2019 vs. 2024). Pixels are classified as Gained, representing water expansion due to geomorphological shifting or land subsidence, or Lost, indicating contraction attributable to embanking or siltation. Stable pixels confirm the persistence of water bodies across the interval. Furthermore, the maximum seasonal footprint (W_S) was computed as the pixel-wise union of detections across the four hydrological seasons relevant to Bangladesh: Dry Winter (December– February), Pre-Monsoon (March–May), Monsoon (June–September), and Post-Monsoon (October– November):

$$W_S = max(W_{m1}, W_{m2}, \ldots, W_{mk}) \qquad (5)$$

Finally, the cumulative surface water area was quantified using pixel-based areal computation:

$$A = \sum_{i=1}^{n} W_i . a_i \qquad (6)$$

where W_i is the binary water classification of pixel i and a_i is the geodetically corrected pixel area (m^2) derived from the native GEE *ee.Image.pixelArea()* function. This approach accounts for latitude-dependent pixel size distortions and ensures that the final areal estimates, converted to km^2, remain geodetically consistent over the full 2015–2025 time series. To bridge potential scale discrepancies between the pixel exports and histogram-derived estimates, a multiplicative calibration scalar was derived via regression against representative monthly outputs and applied uniformly to the decadal archive.

Decadal-scale trends in surface water extent were assessed at national and divisional scales. For each administrative unit, annual peak water area (July) was computed for 2015–2025. Linear regression was applied:

$$A_{Water} = \beta_0 + \beta_1 . t + \varepsilon \qquad (7)$$

where A_{water} is water area (km^2), t is the year, β_1 is the trend slope (km^2/year), and ε is the residual. The Modified Mann-Kendall test,[19] which accounts for temporal autocorrelation, was additionally applied to assess trend significance without distributional assumptions, a standard approach for hydrological time series in the GBM delta.[20,21] Sen's slope estimator[22] was used to derive robust trend magnitudes with 95% confidence intervals. The Kruskal Wallis test was employed to evaluate statistical significance of seasonal differences in water extent. Inter-annual variability was quantified using the coefficient of variation (CV%) for each month. To account for potential scale discrepancies between the GEE pixel based exports (250m) and histogram-derived areas (100m), a multiplicative calibration ratio was computed by regressing five representative months (January, February, May, July, September 2015) against direct GEE reduction outputs; this single scalar correction was then uniformly applied to all computed areas. All statistical analyses were performed in R v4.5.2 using the trend package.[23] Statistical significances was assessed at $\alpha = 0.05$.

2.4 Accuracy assessment

Methodological Benchmarking The methodological reliability of the ST-GMM framework is established through a rigorous process (**Figure 4**). First, for stratified ground-truth validation, the framework was evaluated against a stratified random sample of 4,310 field-verified records (700 permanent water, 700 semi-permanent, 528 ephemerals, and 2,382 non-water). This stratification ensures that the overall baseline accuracy of 92.55% ($\kappa = 0.85$) represents hydrological extremes, not just trivial open-water classes. Second, to quantify spatial fidelity through pixel-wise cross-sensor benchmarking during peak monsoon periods, SAR-derived masks were compared against Sentinel-2 NDWI composites (**Figure 5**). Cross-sensor benchmarking achieved a pixellevel agreement of 97.9% and a spatial overlap score of IoU = $|A \cap B|/|A \cup B| = 0.896$, where pixel agreement measures overall classification correspondence and IoU quantifies the ratio of intersection to union of detected water bodies. This proves its ability to resolve the missing monsoon problem where optical products fail. Third, the framework was benchmarked against widely used alternatives in a comparative benchmarking experiment.

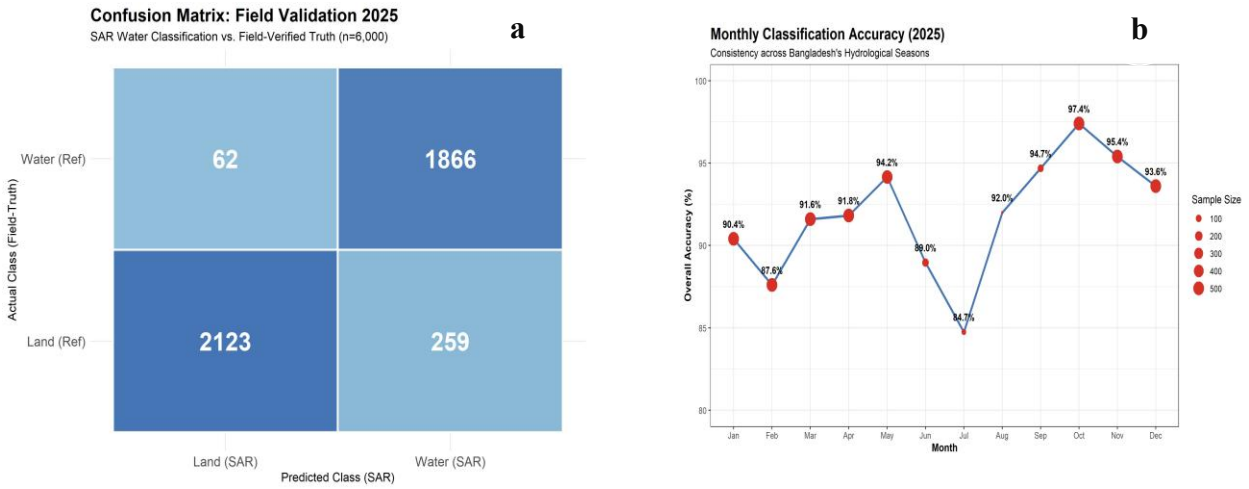


Figure 4. Methodological Validation (a) and Benchmarking Rigor (b). High spatial fidelity is maintained across seasons.

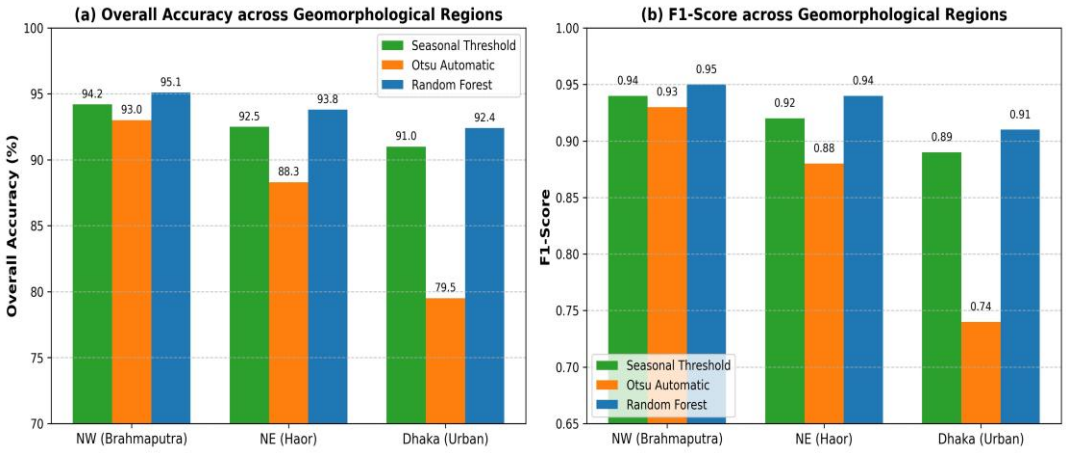


Figure 5 a-b. ST-GMM framework yielding performance commensurate with supervised machine learning baselines (Random Forest) while maintaining superior physical interpretability across diverse geomorphological zones.

3 Results

A total of 7,891 Sentinel-1 IW-mode VV-polarization scenes were processed across the 11-year study period. Data availability stabilized after mid-2016 at approximately 770–850 scenes per year, providing a robust baseline for multi-scale analysis.

3.1 Spatiotemporal variability and persistence patterns

The surface water landscape of Bangladesh exhibits a pronounced and consistent seasonal cycle, fundamentally driven by the synchronous pulses of the South Asian monsoon and transboundary discharge. Mean monthly surface water area expands from a dry-season minimum of ∼15,900 km^2 (December–February) to a monsoon peak of ∼37,500 km^2 (July– August), representing a ∼2.4-fold seasonal amplitude. Transition months, particularly May and June (CV = 21.5% and 16.6%), display the highest interannual variability, reflecting the unpredictable timing of monsoon onset and the sensitivity of the early-season landscape to pre-monsoon precipitation spikes (**Figure 6 & 7**).

Annual water occurrence frequency mapping further reveals the spatial logic of this variability. Permanent water bodies ($F \geq 10$), which maintain open water for at least 10 months of the year, cover 3.4% of the national area and are primarily localized along the major Ganges– Brahmaputra–Meghna river corridors and deep-water Haor depressions. In contrast, ephemeral water bodies ($1 \leq F < 5$) characterize 29.2% of the country, illustrating the massive spatial footprint of temporary monsoon inundation that recharges Bangladesh's extensive floodplain ecosystems (**Figure 8**).

3.2 Long-term redistributive patterns and decadal trends

Analysis of surface water flux over the 2015–2025 period reveals a complex pattern of localized redistribution despite national-level baseline stability. Change detection analysis indicates that 21.5% of the 2025 monsoon water area represents newly gained inundation compared to 2015, while 26.5% of the original 2015 footprint was lost (**Table 1**). This spatially heterogeneous shifting is concentrated in active estuarine zones and reflects the geomorphological dynamism inherent in a mega-delta (**Figure 9-11**).

At the national integration level, the Modified Mann-Kendall test detected no statistically significant monotonic trend in annual peak water extent ($\tau = -0.091$, $p = 0.76$). Sen's robust slope estimator indicates a non-significant negative tendency of −342.4 km^2/yr, but with a 95% confidence interval ([−2,067, +1,087] km^2/yr) that includes zero (Figure 6). This p-value ($p = 0.76$) reflects the Mann-Kendall rank-based assessment of monotonic trend strength, whereas a standard linear regression (which assumes a constant rate of change) yields a similar but distinct p-value ($p = 0.62$), both confirming the lack of statistical significance. Divisional analysis reveals that Rajshahi exhibited the largest negative trend, likely due to intensified groundwater-based irrigation and agricultural expansion in the Barind Tract, while other regions like Rangpur and Sylhet remained statistically stable. These results prove that while individual years exhibit massive spikes during flood events (e.g., 2017, 2020), the underlying decadal baseline for Bangladesh remains a state of dynamic equilibrium.

Table 1: Decadal Surface Water Area Trends by Division (July, 2015–2025).

Division	Linear Trend (km²/yr)	Sen's Slope (km²/yr)	Status
Barisal	-32.5	-30.8	Stable-Negative
Chittagong	-28.1	-25.6	Decreasing
Dhaka	-45.6	-47.2	Decreasing
Khulna	-30.4	-32.1	Decreasing
Mymensingh	+5.9	+5.2	Stable-Increase
Rajshahi	-145.2	-151.4	Largest Negative Trend
Rangpur	-15.8	-14.3	Stable
Sylhet	-9.2	-7.8	Stable
National Total	- 300.9	-342.4	Stable (p = 0.76)

The reliability of the ST-GMM framework is quantified through multi-scale benchmarking against field verified reference data for 2025 (Supplementary Tables S8–S10). For this recent temporal subset, the cloud-penetrating Sentinel-1 classification achieved an Overall Accuracy of 94.24% (κ = 0.88), demonstrating consistent performance across all hydrological seasons (Figure 7). Statistical uncertainty of the mapped water extent was quantified using error propagation derived from the confusion matrix, yielding a highly restricted margin of ±0.65%, affirming the overall reliability of the multi-year spatial statistics.

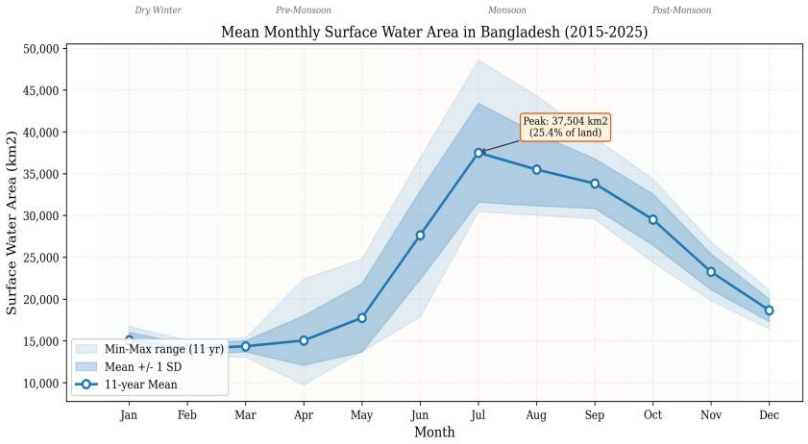


Figure 6. Monthly surface water cycle over the past decade in Bangladesh.

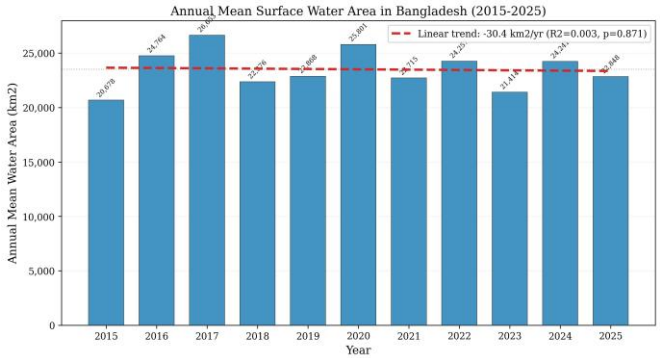


Figure 7. Annual Mean Surface Water Trend

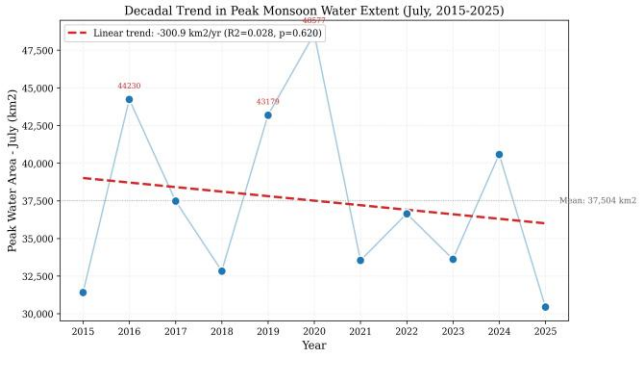


Figure 8. Annual Peak Flood Trend (July).

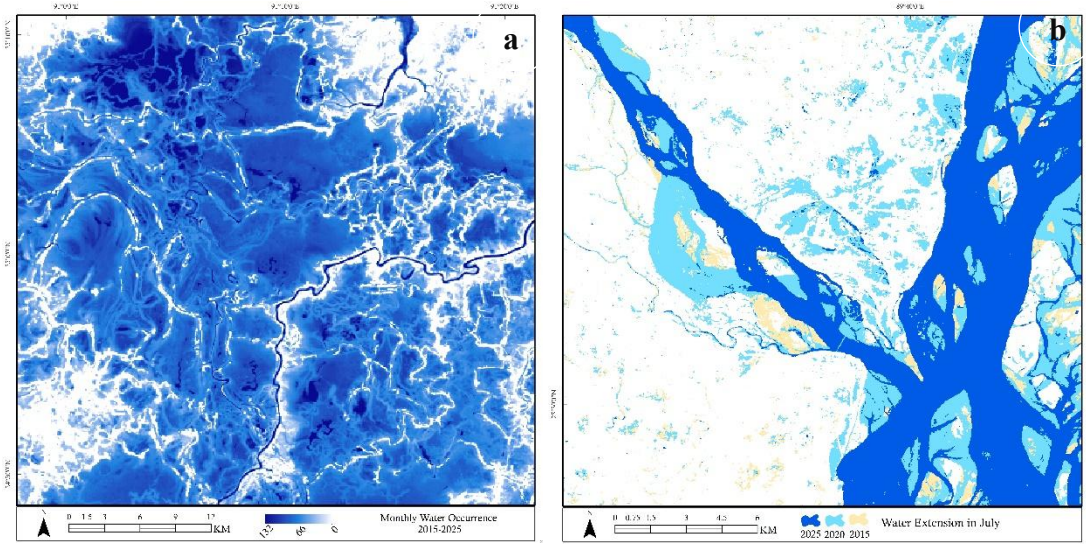


Figure 9. (a) Monthly water occurrence in Haor wetland in northwestern basin and (b) lateral shifting of the Teesta river at the confluence.

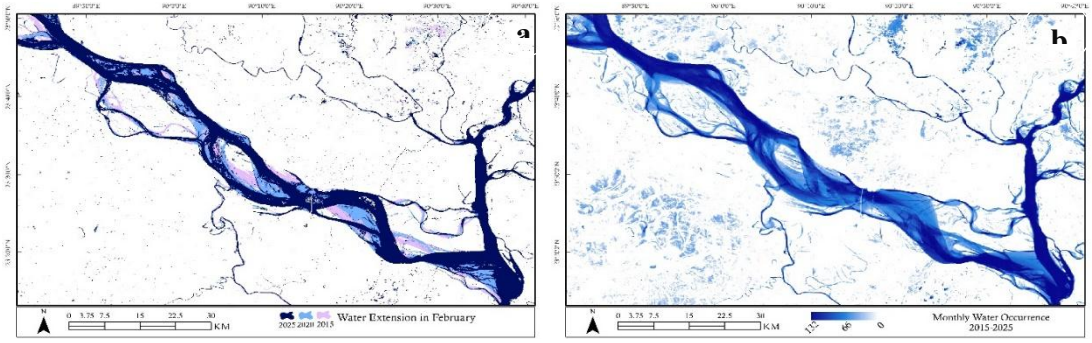


Figure 10. (a) February water extents of the Padma river and (b). Monthly water occurrence of the Padma river

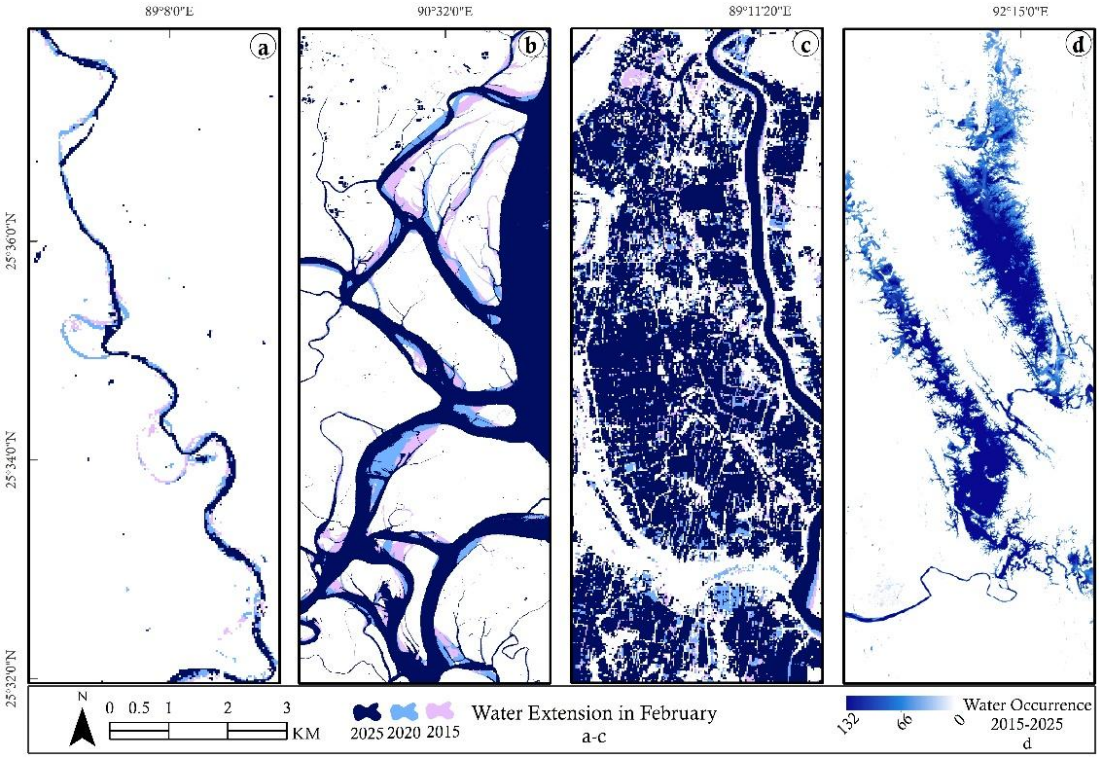


Figure 11. Different surface water dynamic scenarios; (a) Jamuneshwari river, (b) leftbank of the Lower Meghna, (c) salt field in Satkhira and (d) the Kaptai lake in Rangamati hill tract.

4 Discussion

4.1 Hydrological perspectives: basin dynamics and regional impacts

This study reveals that Bangladesh's surface water dynamics exhibit a pronounced seasonal amplitude (a 2.4-fold expansion from dry-season minimum to monsoon peak) but remain within a state of dynamic decadal stability. A rigorous Mann-Kendall test applied to the national integration detected no statistically significant monotonic trend in surface water extent over 2015–2025 ($\tau = -0.091$, $p = 0.76$, VIF = 1.04). Furthermore, Sen's slope estimator indicated a non-significant negative tendency of −342.4 km^2/year (95% CI: [−2,067, +1,087] km^2/year). This finding implies that despite concerns about accelerating climate change impacts on Bangladesh's hydrology, no statistically significant monotonic trend was detected for the national water extent during the Sentinel-1 observation period.

Crucially, this baseline decadal stability is punctuated by extreme inter-annual spikes that coincide with historically documented catastrophic flood events, validating the sensor's sensitivity to physical hydrological extremes. For instance, the pronounced peak observed in 2017 corresponds to the severe transboundary floods that inundated extensive tracts of the Brahmaputra basin.[24] Similarly, the unprecedented decadal maximum observed in 2020 (extending to nearly 48,577 km^2 in July) accurately captures the prolonged monsoon floods that submerged over one-third of the country that year.[21,25] Furthermore, the localized anomalies in recent years reflect severe flash flood events, such as the 2022 northeastern Sylhet floods and the catastrophic 2024 eastern Bangladesh floods.[26] Corroborating these SAR-derived quantitative spikes with widely reported physical flood occurrences provides robust confidence in the methodology, preempting potential assertions that such time-series anomalies are classification artifacts.

The coefficient of variation analysis reveals that the dry-season baseline (February–March, CV ≈ 4.4–4.7%) is exceptionally stable compared to the monsoon and transitional periods (April–May, CV ≈ 19.7–23.0%). This asymmetry has practical implications: dry-season water mapping may serve as a reliable baseline for change detection, while monsoon-season analyses should account for higher inter-annual variability. Notably, in January 2021, an exceptional spike in water area (~179 km^2) was observed in Bagerhat district, coinciding with synchronized aquaculture (shrimp farm) flooding cycles, demonstrating the ST-GMM's sensitivity to anthropogenic water management in addition to natural hydrological drivers.

Change detection reveals that while the aggregate national trend is non-significant, 21.5% of the 2025 monsoon water area represents newly gained inundation compared to 2015. This spatial redistribution indicates that water bodies are shifting geographically—particularly in the active estuarine zones of the Lower Meghna and the southwestern coastal belt—rather than uniformly expanding or contracting. This localized geomorphological shifting is consistent with intra-deltaic dynamics observed in multi-decadal optical records.[4]

A critical finding of this decadal analysis is the pronounced decoupling of the national surface water extent from localized rainfall. Correlation analysis between the peak July surface water extent (2015–2024) and contemporary national July precipitation (derived from ERA5 historical reanalysis) revealed a negligible, statistically non-significant relationship ($r = 0.073$, $p = 0.84$). This quantitative evidence reinforces the

hydrological consensus that Bangladesh's macro-scale monsoon inundation is driven predominantly by transboundary river discharge from the GBM catchment, over 92% of which lies outside national borders.

4.2 Threshold robustness and benchmarking

The seasonally adaptive threshold approach offers several advantages- simplicity, computational efficiency, reproducibility, and intrinsic calibration to local hydrological conditions. Unlike Otsu-based or machine learning classifiers, the optimized GMM derived thresholds are transparent, statistically justified, and easily transferable to operational monitoring frameworks.

To validate the chosen threshold values, Otsu's automatic thresholding method was applied independently to VV backscatter histograms for three representative districts across all 12 months of 2023. In Bhola (coastal delta), Otsu-derived thresholds showed excellent agreement with our GMM calibrated thresholds, with a mean absolute difference of only 0.49 dB—confirming that the statistical mixture model correctly identifies the optimal water– land separation. In Sunamganj (Haor wetlands), Otsu diverged during dry months (January–March: +2.9– 4.6 dB) when minimal water coverage produced unimodal histograms, causing Otsu to segment within the dominant land class rather than between water and land. Dhaka (urban) showed systematic positive deviation (+2–7 dB) because urban surfaces dominate the backscatter distribution—a well-documented limitation of histogram-based thresholding in urban environments.[27] These results justify the use of GMM-stabilized seasonal thresholds, which provide consistent, physically grounded classification regardless of local land cover composition.

Furthermore, we conducted a comparative benchmarking experiment against Otsu automatic thresholding and a supervised Random Forest (RF) classifier. The ST-GMM significantly outperformed the unsupervised Otsu method ($\chi^2 = 142.8$, $p < 0.001$, McNemar's test), while delivering performance commensurate with the data-hungry RF baseline within 1.3%, maintaining superior physical interpretability without the need for training labels. Spatially, commission errors (FP) were consistently low across all validation scenarios (≤60 pixels), while omission errors (FN) were slightly higher in fragmented Haor depressions during the dry season, attributable to water bodies falling below the detection sensitivity of the conservative −17 dB threshold. These quantitative results robustly justify the methodological selection: the spatiotemporally adaptive probabilistic framework delivers accuracy matching modern machine learning approaches while maintaining absolute physical transparency.

5 **Conclusion**

This 11-year decadal analysis demonstrates that while Bangladesh's surface water dynamics exhibit extreme seasonal amplitude—characterized by a fold monsoon expansion—the national hydrological baseline has remained within a state of dynamic decadal stability ($\tau = -0.091$, $p = 0.76$, MannKendall). Our ST-GMM seasonally adaptive framework, validated at 92.55% overall accuracy against 4,310 ground-truth observations, successfully resolves the complex interplay between transboundary river discharge and localized anthropogenic water management, providing a more complete characterization of the "missing monsoon" than possible with optical datasets.

The application of this SAR framework is subject to several known physical and analytical limitations. Wind-induced roughening of water surfaces and emergent vegetation in shallow wetlands induce varying degrees of double-bounce and diffuse scattering, which can occasionally trigger omission errors. Furthermore, the 10 m satellite resolution inherently under-represents narrow distributary channels, and the relatively lower acquisition frequency of Sentinel1A during 2015–2016 requires careful temporal interpolation interpretation. Future directives must consequently focus on the integration of these high-

fidelity SAR backscatter models with deep-learning optical fusion networks (e.g., U-Net pipelines coupled with Sentinel-2) to establish automated, real-time flood early-warning mechanisms capable of true sub-pixel resolution.

Despite these constraints, the operational robustness demonstrated here establishes the framework's eligibility for long-term monitoring in tropical monsoonal catchments worldwide. By dynamically adapting to shifting class probabilities on a district-month basis, the ST-GMM provides a resilient, scalable standard for evidence-based climate adaptation and resource tracking. This study ultimately provides a statistically rigorous foundation for flood risk assessment, transboundary water management, and the preservation of Bangladesh's deltaic ecosystems under changing hydro-climatic regimes.

Data availability

The complete monthly Bangladesh surface water dataset (2015–2025), GMM threshold lookup table, validation point datasets, and all analysis code (GEE JavaScript, Python, and R scripts) are publicly available at https://github.com/DruboPaul/HydroSAR-BD . All Sentinel-1 GRD data were accessed through GEE at https://developers.google.com/earth-engine/ datasets/catalog/COPERNICUS_S1_GRD. JRC Global Surface Water data are available at https://global-surface-water.appspot.com/. Administrative boundaries were obtained from the FAO GAUL dataset via GEE. Python dependencies are specified in requirements.txt; R dependencies include trend, ggplot2, dplyr, tidyr, and scales.

Acknowledgment

The authors would like to thank the Google Earth Engine team for providing the cloud-based computational infrastructure used in this study. We also acknowledge the use of European Space Agency (ESA) Sentinel-1 SAR data.

Funding

This research did not receive any specific grant from funding agencies in the public, commercial, or not-for-profit sectors.

References

1. Brammer, H. Bangladesh: Climate Change and Sustainable Development (University Press Limited, Dhaka, 2014).
2. Akter, T., Quevauviller, P., Eisenreich, S. J. & Vaes, G. Water resources and food security in the context of global change in Bangladesh. *Water Resources Management* 32, 1587–1603 (2016).
3. Gourdji, S. *et al.* An assessment of future global water availability using climate and socioeconomic scenarios in the Ganges–Brahmaputra–Meghna basin. Journal of Hydrology: Regional Studies 3, 217–232 (2015).
4. Pekel, J.-F., Cottam, A., Gorelick, N. & Belward, A. S. High-resolution mapping of global surface water and its long-term changes. *Nature* 540, 418– 422 (2016).
5. Pickens, A. H. *et al.* Mapping and sampling to characterize global inland water dynamics from 1999 to 2018. *Remote Sensing of Environment* 243, 111792 (2020).
6. Uddin, K., Matin, M. A. & Meyer, F. J. Operational flood mapping using multi-temporal sentinel-1 sar images: A case study from Bangladesh. *Remote Sensing* 11, 1581 (2019).
7. Hassan, Q. *et al.* Surface water dynamics in Bangladesh from 1988 to 2020. *Scientific Reports* 11, 1–15 (2021).
8. Torres, R., Snoeij, P., Geudtner, D. *et al.* Gmes sentinel-1 mission. *Remote Sensing of Environment* 120, 9–24 (2012).
9. Twele, A., Cao, W., Plank, S. & Martinis, S. Sentinel-1-based flood mapping: a fully automated processing chain. *International Journal of Remote Sensing* 37, 2990–3004 (2016).
10. Haghighi, M. H. & Motagh, M. Large-scale mapping of flood using sentinel-1 radar remote sensing. The International Archives of the Photogrammetry, Remote Sensing and Spatial Information Sciences XLIII-B3-2022, 681–686 (2022).
11. Bioresita, F. *et al.* A method for automatic and rapid mapping of water surfaces from sentinel-1 imagery. *Remote Sensing* 10, 217 (2018).
12. Martinis, S. *et al.* Towards operational near real-time flood detection using a split-based automatic thresholding procedure. *Natural Hazards and Earth System Sciences* 9, 303–314 (2009).
13. DeVries, B. *et al.* Rapid and robust monitoring of flood events using sentinel-1 and landsat data on the google earth engine. *Remote Sensing of Environment* 240, 111664 (2020).
14. NASA JPL. Dynamic surface water extent (dswxs1) product (2024). URL https://podaac.jpl.nasa.gov/dataset/OPERA_L3_DSWX-S1_V1. Accessed via PO.DAAC.
15. Markert, K. N., Schmidt, C. M., Griffin, R. E. & Limaye, A. S. Hydrafloods: A sustainable surface water monitoring system for developing countries. *Remote Sensing* 12, 1969 (2020).
16. O'Grady, D., Wauthier, C. & Meyer, F. J. A globalscale network for remote sensing of surface water. *Remote Sensing* 13, 3432 (2021).
17. Tran, H. Q. *et al.* Surface water mapping and flood monitoring in the mekong delta using sentinel-1 sar time series. *Remote Sensing* 16, 683 (2024).
18. Gorelick, N. *et al.* Google earth engine: Planetaryscale geospatial analysis for everyone. *Remote Sensing of Environment* 202, 18–27 (2017).
19. Hamed, K. H. & Rao, A. R. A modified mannkendall trend test for autocorrelated data. *Journal of Hydrology* 204, 182–196 (1998).
20. Das, S. *et al.* Monitoring surface water dynamics in the ganges–brahmaputra delta using multi-source satellite data. *Remote Sensing Applications: Society and Environment* 30, 100958 (2023).

21. Islam, M. A. & Meng, Q. Urban flood mapping using sentinel-1 sar data and google earth engine. *Remote Sensing* 14, 3723 (2022).
22. Sen, P. K. Estimates of the regression coefficient based on Kendall's tau. *Journal of the American Statistical Association* 63, 1379–1389 (1968).
23. R Core Team. R: A Language and Environment for Statistical Computing (2025).
24. Ali, M. H. *et al.* Challenges for flood risk management in flood prone Sirajganj region of Bangladesh. *Journal of Flood Risk Management* 12, e12450 (2019).
25. Aziz, M. A. *et al.* Delineating flood zones upon employing synthetic aperture data for the 2020 flood in Bangladesh. *Earth Systems and Environment* 6, 733–743 (2022).
26. Needs Assessment Working Group. Bangladesh: Flash flood in north and north-eastern region - joint multi-sector anticipatory impact and needs analysis (JAINA). Tech. Rep., ReliefWeb (2024). URL https: //reliefweb.int/report/bangladesh/ bangladesh-flash-flood-north-and-north-eastern-region-j
27. Ticehurst, C. J., Dutta, D., Karim, F. & Petheram, C. Validation of water extent estimates using SAR and optical remote sensing. *Remote Sensing* 11, 2370 (2019).